Excitonic cluster model of strongly correlated electronic systems

2000 J. Phys.: Condens. Matter 12 L345

(http://iopscience.iop.org/0953-8984/12/22/103)

J. Phys.: Condens. Matter **12** (2000) L345–L352. Printed in the UK PII: S0953-8984(00)12537-8

LETTER TO THE EDITOR

Excitonic cluster model of strongly correlated electronic systems

Eiichi Hanamura†‖, Nguyen Trung Dan†‡ and Yukito Tanabe§

† Optical Sciences Center, University of Arizona, Tucson, Arizona 85721, USA
‡ ERATO Cooperative Excitation Project, Japan Science and Technology Corporation, Japan
§ Department of Applied Physics, University of Tokyo, Bunkyo-ku, Tokyo 113, Japan

Abstract. An excitonic cluster model is proposed to describe the optical responses of strongly correlated electronic systems, e.g. antiferromagnetic insulators of parent crystals of high-temperature superconductors. This model can take into account both the strong correlation effect of 3d-electrons and the itinerant nature of electronic excitations. Consequently both the electron–hole bound and unbound states can be described on the same footing. As a result, we can resolve the mystery of resonance enhancement of 2-magnon Raman scattering, and remove inconsistencies in the understanding of the absorption spectrum, the photoconductivity spectrum, and large-shift Raman signals.

Competitive behaviour between the strong correlation of 3d-electrons and the itinerant property of doped holes in transition metal oxides of perovskite structure induces a rich variety of transport phenomena such as high-temperature superconductors in cuprates and colossal negative magneto-resistance in manganites. Even in the nondoped crystals, interesting optical responses have been observed, for example, the spin-charge separation in the insulating 1D cuprates and the mystery of the resonance-enhancement spectrum of 2-magnon Raman scattering (RS) in La_2CuO_4 and $YBa_2Cu_3O_6$ [1, 2]. It has been an unsolved problem how to understand and describe the linear and nonlinear optical responses of strongly correlated electronic systems accompanied with propagation effects of optical excitations both in inorganic and organic crystals. In this letter, we propose the excitonic cluster model to solve this problem and show its efficiency by applying it to the insulating cuprates of perovskite-type.

Optical responses of the insulating cuprates without doping originate in the charge-transfer (CT) excitation from the fully occupied O ($2p_\sigma$) electron into the empty level of Cu ($3d_{x^2-y^2}$) in the visible region. Therefore, the 2D network of CuO_2 plays a key role in the optical responses of perovskite-type copper oxides [3, 4]. In addition to this, the electronic ground state is a well-defined antiferromagnetic (AF) insulator [5] and the low-lying elementary excitations can be well described by magnons [6] in a single layer system such as T-type (La_2CuO_4) and T'-type (Gd_2CuO_4, Nd_2CuO_4) and in a double-layer system ($YBa_2Cu_3O_6$) (see figure 1). The correlation energy of Cu ($3d_{x^2-y^2}$) electrons and the energy separation between Cu ($3d_{x^2-y^2}$)- and O($2p_\sigma$)-levels are much larger than the CT t_0 between the nearest neighbour Cu ($3d_{x^2-y^2}$) and O($2p_\sigma$) and t_p between the neighbouring O($2p_\sigma$) orbitals [7]. In the present excitonic cluster model, the electronic excitation in the visible region associated with and without magnetic excitations can be described by making use of this fact. Therefore, we are justified in expanding the optical response functions or the eigen-functions of the optically excited states in terms of t_0 or t_p over the excitation energy in the site-representation. This is one type of

‖ Present address: Chitose Institute of Science and Technology, 758-65 Bibi, Chitose-shi, Hokkaido 066-8655, Japan.

0953-8984/00/220345+08$30.00

degenerate perturbation theory among the group-theoretically adapted basis states of a single particle excitation in the site representation. Indeed, the excitonic cluster model found in this paper is capable of describing quantitatively the absorption spectrum [3, 4], the large-shift RS [8] and the resonance-enhancement of 2-magnon RS [1, 2] as well as two-photon absorption (TPA) spectrum in cuprates of several perovskite types. At the same time we can resolve the mystery of the resonance-enhancement of 2-magnon RS, and clear up the inconsistencies among assignments of the absorption and the photoconductivity spectra [9, 10] as well as the large-shift RS [8].

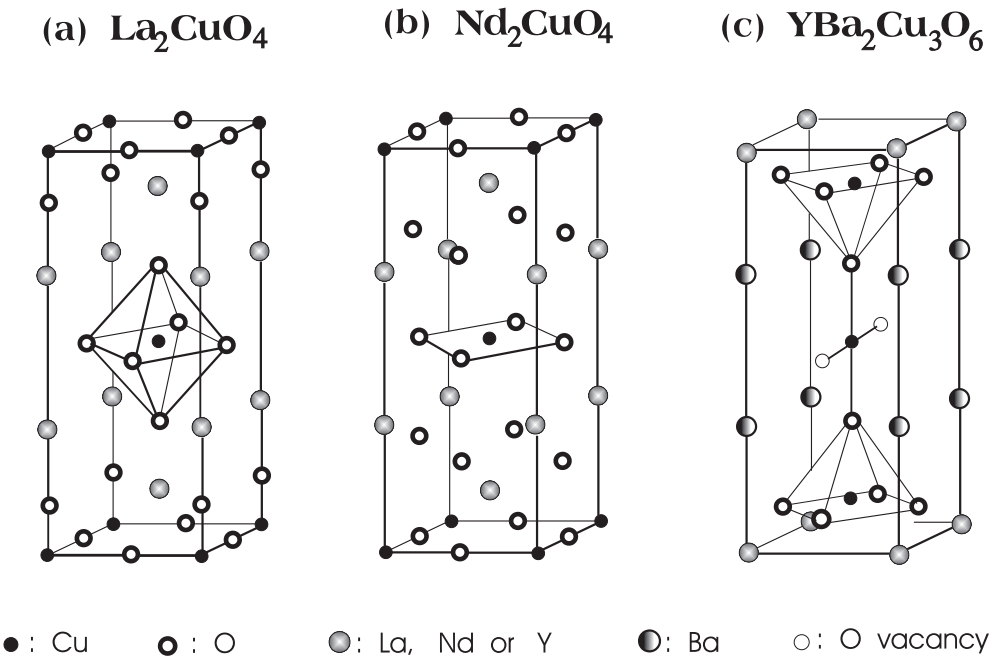

Figure 1. Crystal structures of (a) La_2CuO_4, (b) Nd_2CuO_4, and (c) $YBa_2Cu_3O_6$.

Optical responses of the cuprate crystals mentioned above are described by the following three-band Hubbard Hamiltonian of 2D CuO_2 plane: the O $2p_\sigma$ band ($p_{l\sigma}$, $p^\dagger_{l\sigma}$) with its central energy $E_p + U_p$, singly and doubly occupied Cu $3d_{x^2-y^2}$ bands ($d_{i\sigma}$, $d^\dagger_{i\sigma}$) with E_d and $E_d + U$ as central energies, respectively. This system has the D_{4h} symmetry and is described by

$$H_{el} = \sum_{i,\sigma} E_d d^\dagger_{i\sigma} d_{i\sigma} + \sum_{l,\sigma} E_p p^\dagger_{l\sigma} p_{l\sigma} + H'_{el} + U \sum_i d^\dagger_{i\uparrow} d_{i\uparrow} d^\dagger_{i\downarrow} d_{i\downarrow} + U_p \sum_l p^\dagger_{l\uparrow} p_{l\uparrow} p^\dagger_{l\downarrow} p_{l\downarrow} + V \sum_{i\sigma\sigma'} \sum_{l\in\{i\}} d^\dagger_{i\sigma} d_{i\sigma} p^\dagger_{l\sigma'} p_{l\sigma'} \quad (1)$$

$$H'_{el} = t_0 \sum_{i\sigma} \sum_{l\in\{i\}} d^\dagger_{i\sigma} p_{l\sigma} + t_p \sum_{l\sigma} \sum_{l'\in\{l\}} p^\dagger_{l\sigma} p_{l'\sigma}. \quad (2)$$

Here U and U_p are the on-site Coulomb repulsions at the Cu and O sites, respectively, and V is the nearest neighbour Cu–O interatomic Coulomb repulsion. The first and second terms of H'_{el} (equation (2)) bring in, respectively, the hybridization between the nearest neighbour Cu and O orbitals ($l \in \{i\}$ in equation (2)), and that between the two nearest neighbour oxygen orbitals ($l' \in \{l\}$ in equation (2)). The electronic ground state of this Hamiltonian has one

electron ($3d_{x^2-y^2}$) per Cu^{2+} ion and has fully occupied 2p electrons per O^{2-} ion surrounding this Cu^{2+} ion. The ground state $|g\rangle$ is represented in site-representation as follows:

$$|g\rangle \equiv \prod_{m+n=\text{even}}^{A} d_{\uparrow}^{\dagger}(2m,2n) \prod_{m+n=\text{odd}}^{B} d_{\downarrow}^{\dagger}(2m,2n) \prod_{m+n=\text{odd}} p_{\uparrow}^{\dagger}(m,n)\, p_{\downarrow}^{\dagger}(m,n)\,|0\rangle \tag{3}$$

where the vacuum $|0\rangle$ is defined by the product of whole $O(2p)^4$ and $Cu(3d)^8$ in which two $2p_\sigma$ electrons and two $3d_{x^2-y^2}$ electrons are missing, respectively.

The radiation field can induce the CT excitations through the transition dipole moment $\boldsymbol{\mu}_{il}$ which is linearly proportional to t_0 and also to the unit vector drawn from the ith lattice point to the lth one. The CT excitation $\psi^A(1,0) = d_{A\downarrow}^{\dagger}(0,0)\, p_{x\downarrow}(1,0)\,|g\rangle$ represents formation of a bound CT exciton with the 'electron' $(3d_{x^2-y^2})^2$ at the A-sublattice Cu (0,0) and the 'hole' $(2p)^5$ at O (1,0) as shown in figure 2(a). When two electrons of $O(2p_x\ \uparrow)$ at (1,0) and $Cu(3d_{x^2-y^2}\ \downarrow)$ at the B-sublattice (2,0) are exchanged through the second order process in t_0, the state $\psi^A_{(2,0)}(1,0) = d_{A\downarrow}^{\dagger}(0,0)\, p_{x\uparrow}(1,0)\, d_{B\uparrow}^{\dagger}(2,0)\, d_{B\downarrow}(2,0)\,|g\rangle$ is created as shown in figure 2(b). Here the argument (1,0) of $\psi^A_{(2,0)}(1,0)$ also describes the location of a 'hole' O^- (now with its down spin) and the suffix (2,0) gives that of the reversed Cu^{2+} spin in the B-sublattice.

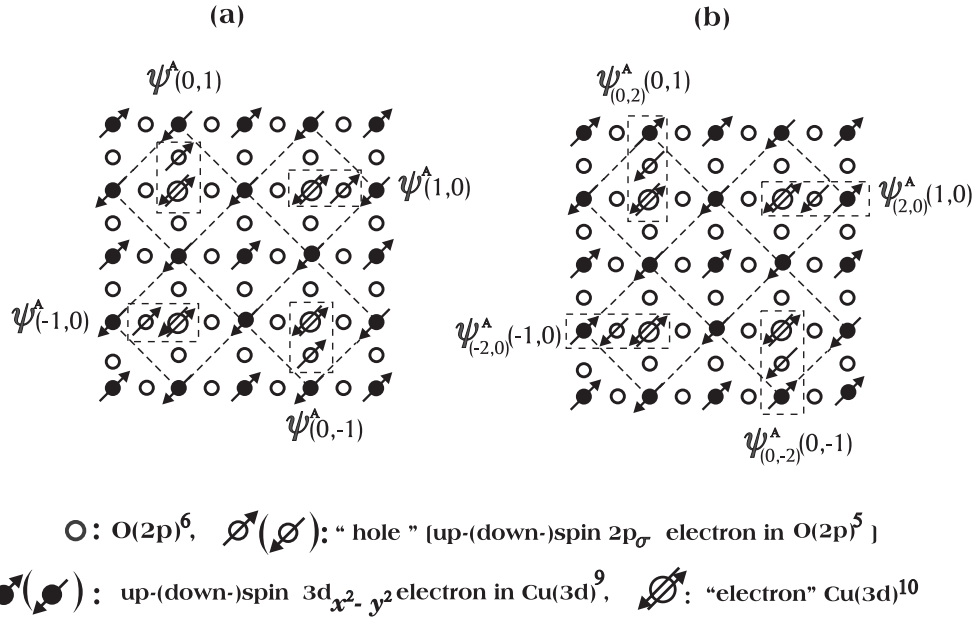

Figure 2. Charge-transfer excitations around A-sublattice. (a) Dipole-allowed excitons and (b) 2-magnon excitations.

Reflecting the D_{4h} symmetry of the CuO_2 plane, we have four equivalent CT excitations: $\psi^{A(B)}(1,0)$, $\psi^{A(B)}(0,1)$, $\psi^{A(B)}(-1,0)$ and $\psi^{A(B)}(0,-1)$ around the A-(B-)sublattice Cu ions, corresponding to four diagrams in figure 2(a). Four dipole-allowed states around the A-sublattice are mixed with each other by the second-order process in t_0, i.e. $t_1 = t_0^2/(U - U_p - E_p - V)$ and t_p. When we diagonalize the energy matrix, we have the eigen-functions and eigen-energies with the A_{1g}, B_{1g} and $E_u^x(E_u^y)$ representation of the D_{4h} symmetry. Here the diagonal energy E_0 is evaluated to the fourth order in t_0, i.e. the superexchange energy

J in addition to the second order exchange energy $-t$. Only the states with $E_u^{x,y}$-symmetry (Ψ^1_{exA} and Ψ^1_{eyA}) can contribute to the absorption and 2-magnon RS [11]. The states $A_{1g}(\Psi^1_{aA})$ and $B_{1g}(\Psi^1_{bA})$ are observable in the TPA spectrum, and the large-shift RS in which the incident light frequency ω is much larger than the excitation energy $E(B_{1g})$ and $E(A_{1g})$.

Only the states with the same symmetry in the site representation are intermixed with each other through H'_{el} (equation (2)). Therefore, we may consider the states $\Psi^m_{exA}(n)$ as the bases which give the effects of CT, e.g. on the absorption and 2-magnon RS. Here the superscript m denotes the distance between the 'electron' at the origin and the 'hole', while the argument n stands for the separation between the reversed spin and the 'hole', and the argument (0) represents the case of the nearest neighbour and no argument indicates the case without reversed spin. For example, the same second-order exchange t described above induces the state $\Psi^1_{exA}(0)$ as a linear combination of $\psi^A_{(2,0)}(1,0)$ and $\psi^A_{(-2,0)}(-1,0)$ shown in figure 2(b), and Ψ^n_{exA} (with $n \geqslant 2$) means the unbound states of the 'electron' and the 'hole'. Furthermore, only the symmetrical states with respect to the interchange of the A- and B-sublattices can contribute to the optical responses. As a result, the eigen-states belonging to eigen-energy E_i of the CT excitation are represented as a symmetrical linear combination of the states with the same symmetry species, e.g. for dipole-allowed states:

$$\Psi_{ex+}[i] = a_i\Psi^1_{ex+} + b_i\Psi^1_{ex+}(0) + c_i\Psi^1_{ex+}(2) + d_i\Psi^1_{ex+}(1) + e_i\Psi^2_{ex+} + f_i\Psi^2_{ex+}(0) + g_i\Psi^3_{ex+} + h_i\Psi^3_{ex+}(0) + \cdots \tag{4}$$

where

$$\Psi^n_{ex+} = \frac{1}{\sqrt{2}}\left\{\Psi^n_{exA} + \Psi^n_{exB}\right\} \qquad \Psi^n_{ex+}(i) = \frac{1}{\sqrt{2}}\left\{\Psi^n_{exA}(i) + \Psi^n_{exB}(i)\right\}.$$

The eigen-energies are numbered from the low-energy side. We have also repeated this procedure for the A_{1g} and B_{1g} representations of the D_{4h} symmetry.

We calculate the off-diagonal matrix elements of H'_{el} to the second-order in t_0 and the first-order in t_p between these basis states for $E^x_u(E^y_u)$, A_{1g} and B_{1g}, and diagonalize these matrices separately. Note that the bases in equation (4) are the states with a single 'electron' and 'hole' excitation while the intermediate states in evaluating the effects of H' are states with two or zero pairs of excitation. The imaginary part of the dielectric function $\varepsilon_2(\omega)$ which is proportional to the linear absorption spectrum $\alpha(\omega)$ is derived as

$$\varepsilon_2^{xx}(\omega) = 4\pi N_u\mu_x^2 \sum_{i=1} \frac{\Gamma_i(a_i)^2}{(E_i-\omega)^2+\Gamma_i^2} \tag{5}$$

with N_u indicating the number density of the unit cells and Γ_i representing the relaxation constant of the ith level. The resonant-enhancement spectrum of 2-magnon RS is described by the absolute square of Raman-tensor [11]:

$$\chi_{xx}(\omega) = 2|\mu_x|^2 \sum_{i=1} \frac{a_i(b_i-c_i)}{E_i-\omega-i\Gamma_i} \tag{6}$$

where ω denotes the angular frequency of incident radiation field. In equations (5) and (6), E_i stands for the eigen-energy of the dipole-allowed states $\Psi_{ex+}[i]$. Thus the optical responses in which we are interested are described by the coefficients a_i, b_i, c_i of $\Psi_{ex+}[i]$ for only several lowest eigen-energies in the visible region as realized from equations (5) and (6). The convergence of $\varepsilon_2(\omega)$ and $\chi_{xx}(\omega)$ against the number of basis functions is so excellent that $n = 4(n = 5)$ is enough for Gd_2CuO_4, Nd_2CuO_4 and La_2CuO_4 ($YBa_2Cu_3O_6$). This is because the perturbation expansion in t_0 is well justified as $t_0/(U-E_p-U_p)$ and $t_0/(E_p+U_p)$ are much smaller than one (see material constants shown in table 1). Here, t_0, t_p and V are

determined so as to fit the spectrum $\varepsilon_2(\omega)$ to the observed one. Both the experimental and the theoretical $\varepsilon_2(\omega)$ are compared in figure 3. Here the values of t_0 and t_p are found to be in good agreement with the results of the first-principle calculation [12] except for t_p of Nd_2CuO_4, and the relaxation rates could be fixed by assuming the Lorentzian shape: $\Gamma_{1,2} = 0.32$ eV, $\Gamma_{i\geqslant 3} = 0.34$ eV (La_2CuO_4), $\Gamma_{1,2} = 0.32$ eV, $\Gamma_{i\geqslant 3} = 0.36$ eV ($YBa_2Cu_3O_6$) and $\Gamma_1 = 0.25$ eV, $\Gamma_{i\geqslant 2} = 0.44$ eV (Gd_2CuO_4 and Nd_2CuO_4). The dependence of the calculated spectra on the material constants can be briefly discussed as follows. First, the position of the strongest absorption peak depends mainly on the values of parameters U, U_p, E_p in the form of the CT excitation energy $U-U_p-E_p$. The value of this energy has been determined from comparisons of the position of the observed strongest absorption peak with that of the calculated. The values of U_p and E_p have been chosen almost commonly from the first-principle calculations as given in table 1. At the same time, we find that the broadening as well as the relative intensities of the absorption peaks are mainly governed by the values of t_p, t_0 and V. When t_p is substantially small in comparison with t_0, the first two energy levels are largely separated (for example, in Gd_2CuO_4 and Nd_2CuO_4, $E_2 - E_1 = 0.45$ eV) and the intensity of the strongest absorption peak is contributed mainly by the first state. If t_p is close to $t_0/2$, the two levels become closer (for example, in La2CuO$_4$ and $YBa_2Cu_3O_6$, $E_2 - E_1 \sim 0.1$ eV) and the intensity of the strongest peak comes mainly from the two first states. Besides, the relative values of t_p and V have an important role in determining the relative intensity of the absorption peak and the shoulder or the second peak as shown in table 1 and figure 3. Second, if we vary all parameters in a region around the values given in table 1, we would obtain spectra having similar shapes, but the best fits are obtained by choosing parameters given in table 1 as well as the set of Γ_i given above. Details of the calculation will be given in a separate publication.

Table 1. Material constants (in eV).

	U	U_p	E_p	t_0	t_p	V	J
La_2CuO_4	10.0	3.5	3	0.82	0.4	0.5	0.14
$YBa_2Cu_3O_6$	10.0	3.4	3	1.0	0.55	0.35	0.12
Gd_2CuO_4	9.65	3.4	3	0.85	0.3	0.4	0.15
Nd_2CuO_4	9.62	3.4	3	0.85	0.3	0.4	0.13

Let us resolve the mystery of why 2-magnon RS has been observed not to be enhanced even when the incident light frequency ω approaches the strongest absorption peak with the lowest excitation energy, but instead it is resonantly enhanced for ω close to the weak shoulder or the second peak on the high energy side as shown in figures 3(a) and 3(b) for La_2CuO_4 and $YBa_2Cu_3O_6$, respectively. To explain this mystery, Chubukov and Frenkel [13] proposed the band-to-band transition model of the Mott–Hubbard system in which the Raman tensor is expanded to the second order in the intraband fermion-magnon interaction. They found multiple-resonance to be responsible for the enhancement on the high-energy side. However, the CT between the Cu- and O-ions and the excitonic effect were completely neglected in their treatment. On the contrary, these are the main issue in our treatment and we find that this mystery can now be resolved within this model as shown in figures 3(a) and 3(b). In the present treatment the interaction between the dipole-allowed excitation Ψ^1_{ex+} in figure 2(a) and the 2-magnon excitation $\Psi^1_{ex+}(0)$ in figure 2(b) is so strong that this has been diagonalized at first in equation (4) without resorting to the conventional perturbation expansion. This is due to the fact that the 2-magnon RS is so strongly observed. The contribution to $\chi_{xx}(\omega)$ from the mainly dipole-allowed component Ψ^1_{ex+} at E_2 is almost cancelled out by the mainly 2-magnon excited states $\Psi^1_{ex+}(0)$ and $\Psi^2_{ex+}(0)$ at E_1 and E_3 through the destructive interference.

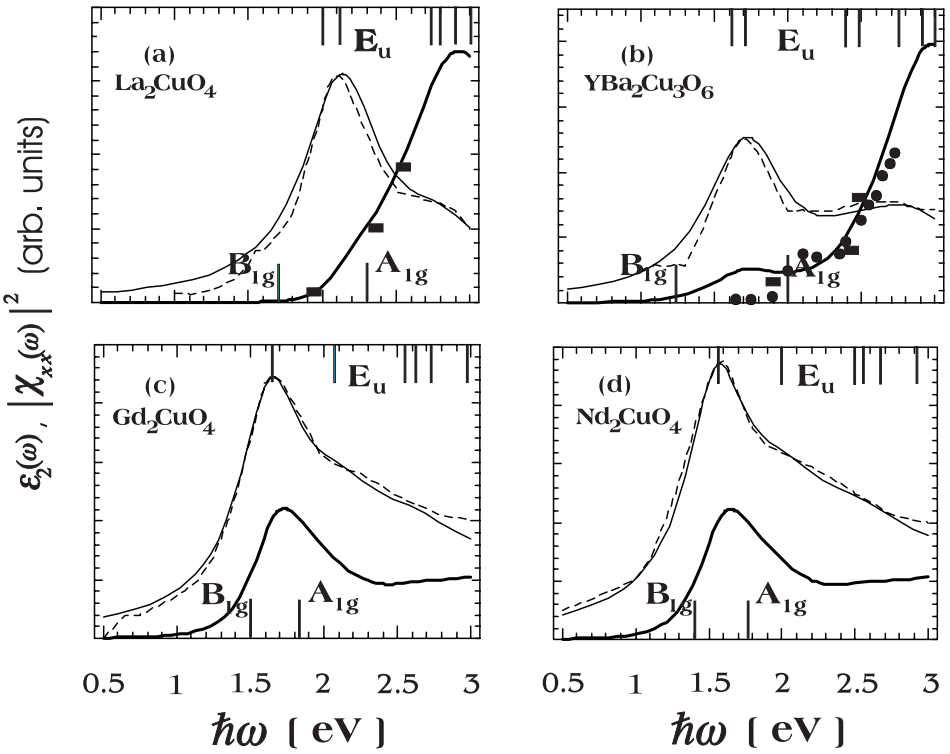

Figure 3. Absorption spectra of theoretical (thin lines) and experimental (dotted lines [3,4]) $\varepsilon_2(\omega)$, and enhancement spectra of 2-magnon RS of theoretical (solid lines) and experimental (filled rectangles [1] and circles [2]) $|\chi_{xx}(\omega)|^2$ of (a) La_2CuO_4, (b) $YBa_2Cu_3O_6$, (c) Gd_2CuO_4 and (d) Nd_2CuO_4. The large-shift RS gives good agreement of calculated (vertical bars on the bottom line) B_{1g} and A_{1g} modes with the observed ones [8] under modified assignments.

The higher energy levels $E_{i\geqslant 3}$ which correspond to the motion of the unbound electron–hole pair contribute additively to the Raman tensor in equation (6), so that the 2-magnon RS is resonantly enhanced for $\omega \geqslant E_3$ as shown in figures 3(a) and 3(b). The above cancellation comes physically from the strong hybridization between $\Psi^1_{ex+}(0)$ and $\Psi^2_{ex+}(0)$ through the CT between the nearest neighbour oxygen ions t_p, which pushes one of these levels down below the mainly dipole-allowed state. This is not the case for Gd_2CuO_4 and Nd_2CuO_4 which are without the apical oxygens as shown in figure 1(b). Here the effective CT t_p between the nearest neighbour oxygens on the CuO_2 plane is expected to be reduced very much because the indirect channels of t_p through the apical oxygen $2p_z$ orbitals are closed [14]. This is in contrast to the cases of La_2CuO_4 (figure 1(a)) and $YBa_2Cu_3O_6$ (figure 1(c)). As a result, the exchange splitting 0.45 eV on the order of $2t$ between the dipole allowed Ψ^1_{ex+} and the 2-magnon excited state $\Psi^1_{ex+}(0)$ remains larger than the broadening $\Gamma = 0.25$ eV for Gd_2CuO_4 and Nd_2CuO_4. As a result, we may expect the resonance-enhancement of 2-magnon RS to be observable for ω close to the lowest CT exciton as also shown by the solid lines in figures 3(c) and 3(d).

Next, let us clear up the inconsistency about the assignments of the absorption and photo-conductivity spectra, and the large-shift Raman scattering lines. Although the absorption spectrum of La_2CuO_4 was analysed by the exciton model, the photo-conductivity was observed

to rise at the same frequency as the absorption peak and the bound state of exciton was denied [9]. The same conclusion was also derived for $YBa_2Cu_3O_6$ [10]. This inconsistency may be removed by the present excitonic cluster model in which both the bound and unbound states are treated on the same footing. The lowest energy state E_1 of both La_2CuO_4 and $YBa_2Cu_3O_6$ consists mainly of the 2-magnon excited states $b_1 = -0.62(0.53)$ and the unbound state $e_1 = -0.46(0.47)$ for $La_2CuO_4(YBa_2Cu_3O_6)$. The second lowest state E_2 is mainly the bound dipole-allowed state $a_2 = 0.77(0.60)$. This result is sensitive to the relative magnitude of $t_p = 0.55$ eV (0.3 eV) to $V = 0.35$ eV (0.4 eV) as well as to $t_0 = 1.00$ eV (0.85 eV) for $YBa_2Cu_3O_6$ (Nd_2CuO_4 and Gd_2CuO_4). Therefore, for $YBa_2Cu_3O_6$ and also for La_2CuO_4, we may understand that the absorption is induced mainly by the second lowest level E_2 while the photo-conductivity is carried by the lowest-states accompanied with 2-magnon excitations and electron–hole separation. The story is quite different for Nd_2CuO_4 and Gd_2CuO_4. Here the lowest level E_1 is a bound CT exciton and the second lowest level E_2 is separated by about the exciton binding energy $V = 0.4$ eV or the exchange energy $2t = 0.45$ eV above E_1. Observation of the photo-conductivity spectrum rising above E_2 for Nd_2CuO_4 and Gd_2CuO_4 will also confirm the present theoretical result.

The CT excitons with the B_{1g}, A_{1g}, A_{2g} and B_{2g} representations of the D_{4h} symmetry are observable in the large-shift RS and TPA spectra. We have calculated the eigen-states and eigen-energies of B_{1g} and A_{1g} representations by making the basis states $\Psi^m_{a+}(n)$ and $\Psi^m_{b+}(n)$, evaluating the matrix elements of H'_{el} (equation (2)) among these bases and diagonalizing these matrices separately. Then as shown on the bottoms of figures 3(a)–(d), these eigen-energies are found to be in agreement with the observed energies [8] under modified assignments.

In conclusion, we have been able to understand quantitatively the characteristics of several optical responses which depend sensitively on the relative values of t_p and V. This also seems to clear up the inconsistent assignment [9] of the photo-conductivity spectrum [9, 10], the absorption spectrum [3, 4, 9], and the large-shift RS [8]. Finally, we have resolved the mystery of the resonance-enhancement spectrum of 2-magnon RS. We believe that the excitonic cluster model will be able to describe the linear and nonlinear optical responses of the strongly correlated electronic system effectively in general including both organic and inorganic crystals.

One of the authors (EH) thanks Professor M V Klein, Professor Y Tokura, and Professor S Uchida for fruitful discussions and important information relevant to the present calculation.

References

[1] Yoshida M, Tajima S, Koshizuka N, Tanaka S, Uchida S and Itoh T 1992 *Phys. Rev.* B **46** 6505
[2] Blumberg G, Abbamonte P, Klein M V, Lee W C, Ginsberg D M, Miller L L and Zibold A 1996 *Phys. Rev.* B **53** R11930
[3] Tokura Y, Koshihara S, Arima T, Takagi H, Ishibashi S, Ido T and Uchida S 1990 *Phys. Rev.* B **41** R11657
[4] Arima T, Kikuchi K, Kasuya M, Koshihara S, Tokura Y, Ido T and Uchida S 1991 *Phys. Rev.* B **44** R917
[5] Keimer B, Belk N, Birgeneau R J, Cassanho A, Chen C Y, Greven M, Kastner M A, Aharony A, Endoh Y, Erwin R W and Shirane G 1992 *Phys. Rev.* B **46** 14034
[6] Lyons K B, Fleury P A, Schneemeyer L F and Waszczak J V 1988 *Phys. Rev. Lett.* **60** 732
Lyons K B, Sulewski P E, Fleury P A, Carter H L, Cooper A S, Espinosa G P, Fish Z and Cheong S-W 1989 *Phys. Rev.* B **39** R9693
[7] Mattheiss L F and Hamann D R 1989 *Phys. Rev.* B **40** 2217
[8] Salamon D, Liu R, Klein M V, Karlow M V, Cooper S L, Cheong S-W, Lee W C and Ginsberg D M 1995 *Phys. Rev.* B **51** 6617
[9] Falck J P, Levy A, Kastner M A and Birgeneau R J 1992 *Phys. Rev. Lett.* **69** 1109

[10] Yu G, Lee C H, Mihailovic D and Heeger A J 1993 *Phys. Rev.* B **48** 7545
[11] Hanamura E, Tanabe Y and Dan N T 1999 *J. Luminescence* **83/84** 19
[12] Mizuno Y, Tohyama T and Maekawa S 1998 *Phys. Rev.* B **58** R14713
[13] Chubukov A V and Frenkel D M 1995 *Phys. Rev. Lett.* **74** 3057
[14] Matsukawa H and Fukuyama H 1989 *J. Phys. Soc. Japan* **58** 2845